Oxidative stress-induced ubiquitination of RCAN1 mediated by SCF$^{ß\text{-}TrCP}$ ubiquitin ligase

SACHIE ASADA[1], AKEMI IKEDA[1], RINA NAGAO[1], HIROSHI HAMA[2], TATSUHIKO SUDO[3], AKIYOSHI FUKAMIZU[4], YOSHITOSHI KASUYA[5] and TSUTOMU KISHI[1]

[1]Kishi Initiative Research Unit, Frontier Research System, [2]Laboratory for Cell Function Dynamics Advanced Technology Development Group, Brain Science Institute, [3]Antibiotics Laboratory, RIKEN, 2-1 Hirosawa, Wako, Saitama 351-0198; [4]Center for Tsukuba Advanced Research Alliance, University of Tsukuba, 1-1-1 Tennoudai, Tsukuba, Ibaraki 305-8577; [5]Department of Biochemistry and Molecular Pharmacology, Graduate School of Medicine, Chiba University, 1-8-1 Inohana, Chuo-ku, Chiba 260-8670, Japan

Received February 1, 2008; Accepted March 21, 2008

Abstract. A change in the protein level of RCAN1 (DSCR1/MCIP/Adapt78/CSP1) has been implicated in oxidative stress-induced cell death in neurons and in the pathogenesis of Alzheimer's disease. The pathogenic processes in neurodegenerative diseases are closely related to oxidative stress and the ubiquitin proteasome system (UPS). Therefore, we investigated whether oxidative stress induces a change in the protein level of RCAN1 through the UPS. H_2O_2 induced ubiquitination of RCAN1 at the same concentrations as those causing a decrease in RCAN1 in HEK293T cells. ß-TrCP, the F-box protein component of SCF ubiquitin ligase, interacted with RCAN1 in response to H_2O_2 stimulation. Although FBW4, another F-box protein, interacted with RCAN1, its interaction was independent of H_2O_2 stimulation. *In vitro* ubiquitination assay showed that SCF$^{ß\text{-}TrCP}$ but not SCF^{FBW4} increased ubiquitination of RCAN1, dependent on H_2O_2 stimulation. In addition, knockdown of ß-TrCP by siRNA abolished the H_2O_2-induced decrease in RCAN1 in HEK293T cells. We further examined whether RCAN1 undergoes ubiquitination by H_2O_2 in primary neurons, similarly to that in HEK293T cells. An H_2O_2-induced decrease in RCAN1 was exhibited also in hippocampal and cortical neurons. Ubiquitination of RCAN1 was induced by 500 μM H_2O_2, the concentration at which H_2O_2 induced a decrease in RCAN1 in primary neurons. These results suggest that H_2O_2 induces SCF$^{ß\text{-}TrCP}$-mediated ubiquitination of RCAN1, leading to a decrease in the protein level of RCAN1.

Correspondence to: Dr Tsutomu Kishi, Kishi Initiative Research Unit, Frontier Research System, RIKEN, 2-1 Hirosawa, Wako, Saitama 351-0198, Japan
E-mail: tkishi@riken.jp

Key words: RCAN1, SCF$^{ß\text{-}TrCP}$, ubiquitin, oxidative stress, neuron

Introduction

The physiological and pathological roles of regulators of calcineurin (RCAN) 1 (also known as DSCR1/MCIP/Adapt78/CSP1) have been studied based on its gene locus, mRNA expression profile and protein function. The RCAN1 gene is located at 21q22.12, near the Down syndrome critical region on human chromosome 21, and consists of seven exons (1,2). The RCAN1 transcript is generated by alternative first exon splicing (exon 1-4), resulting in four different mRNA isoforms (2). Two of these isoforms, RCAN1-1 and RCAN1-4, are mainly expressed and are detected in several tissues, including the brain and heart (2-4).

RCAN1 interacts with important signaling molecules; calcineurin (Cn), integrin αvß3 and Raf-1 (5-9). The function of RCAN1 in relation to Cn, among the interacting molecules, has been the most well defined. Cn is a serine/threonine phosphatase consisting of a catalytic A subunit (CnA) and a regulatory B subunit (10-13). RCAN1, through either the N-terminal or C-terminal region, binds to CnA and inhibits Cn activity *in vitro* (5,7,14). Overexpression of RCAN1 in transgenic mice exhibits an inhibitory effect on Cn activity, as expected from *in vitro* studies (15,16). However, analysis of RCAN1 knockout mice by several groups demonstrated that RCAN1 led to facilitation and/or suppression of CnA activity under physiological and pathological conditions in each knockout mouse (17-20). The precise mechanism of CnA regulation by RCAN1 *in vivo* remains obscure.

Ubiquitin is a 76-amino acid polypeptide that is conjugated to lysine residues of the target protein (21,22). Conjugation of the poly-ubiquitin chain occurs through sequential steps catalyzed by a ubiquitin-activating enzyme (E1), ubiquitin-conjugating enzyme (E2) and ubiquitin-protein ligase (E3) (23,24). The poly-ubiquitinated protein is recognized by 26S proteasome, followed by degradation (24,25). E3s, which

have been classified into various types, are responsible for recognition of the specific substrate. SCF (Skp1/Cullin/F-box protein) ubiquitin ligase, one of the RING-type E3s, recognizes phosphorylated substrate through the binding of F-box protein to phosphorylation sites of the substrate (24,26-28). The ubiquitin-proteasome system (UPS) is implicated in the regulation of normal protein levels in response to cellular conditions and in the clearing of defective proteins. Impairment of the UPS causes deposition of ubiquitinated and aberrant proteins, resulting in cellular dysfunction. Studies indicate that impairment of the UPS is linked to the pathogenesis of neurodegenerative diseases, such as Alzheimer's (AD), Parkinson's and polyglutamine disease (29,30).

Oxidative stress increases defective proteins and induces various cytotoxicity in cells, which is closely related to the pathogenic processes in neurodegenerative diseases (31,32). A change in RCAN1 protein level is detected in the brain of AD, and neurons in RCAN1 knockout mice exhibit resistance to cell death by oxidative stress (19,33). These findings suggest that a change in RCAN1 protein level may be required for a cellular response to oxidative stress. Recently, we and others demonstrated that a *Saccharomyces cerevisiae* ortholog of RCAN1 is ubiquitinated by a rise in intracellular Ca^{2+}, and exogenously expressed human RCAN1-4 is ubiquitinated in normal culture conditions (34-36). Moreover, oxidative stress induces a decrease in RCAN1-4 via an MG132-sensitive pathway in HeLa cells (37). Taken together, these findings raise the possibility that oxidative stress may induce a ubiquitin-mediated decrease in the protein level of RCAN1. However, the precise mechanism of UPS regulation of the protein level of RCAN1 under oxidative stress remains unclear. Likewise, especially in neurons, whether RCAN1 is ubiquitinated under oxidative stress is unknown.

In the present study, we investigated whether RCAN1 undergoes ubiquitination in response to oxidative stress in HEK293T cells and primary neurons to gain further insight into the regulation of the RCAN1 protein level.

Materials and methods

Materials. PD150606 was purchased from Calbiochem (Nottingham, UK). MG132 was from Peptide Institute Inc. (Osaka, Japan). Anti-FLAG M2, anti-α-tubulin and anti-GAPDH antibodies were from Sigma (St. Louis, MO). Anti-HA (3F10 and 12CA5), anti-multi-ubiquitin, anti-lamin A/C and anti-neuronal class III ß-tubulin (TUJ1) antibodies were from Roche (Mannheim, Germany), MBL (Nagoya, Japan), Cell Signaling Technology (Beverly, MA) and Covance (Berkeley, CA), respectively.

Anti-RCAN1 antibodies. GST-human RCAN1-1 and its deletion mutant comprising amino acids (aa) 1-83 were expressed in Rosetta-gami 2 competent cells (Novagen, Madison, WI), and then purified recombinant GST proteins were used to immunize rabbits. Polyclonal antibodies were raised, and serum from the immunized rabbits was affinity purified commercially (Tanpaku Seisei Kogyo, Gunma, Japan). Anti-RCAN1.2 antibody was purified on a GST-RCAN1-1 affinity column. Anti-RCAN1.3 antibody was isolated through a two-step purification process: Antiserum was passed over a GST-RCAN1-1 (aa 1-83) affinity column, and the flow-through from the column was then purified on a GST-RCAN1-1 affinity column.

Cell culture. HEK293T cells were cultured in Dulbecco's modified Eagle's medium (DMEM) (Nissui Pharmaceutical Co., Tokyo, Japan) supplemented with 10% fetal bovine serum (Cansera International Inc., Ontario, Canada). In the case of non-transfection samples, cells were plated at $3x10^4$ cells in 24-well plates and cultured for 24 h. Primary cultures of hippocampal and cortical neurons were performed as previously described with minor modification (38,39). Briefly, the hippocampus and cortex were dissected from the mouse brain on embryonic day 17 and incubated in dissociation solution [Earle's balanced salt solution containing 10 U papain (Sigma) and 1 mM KYN (Sigma)] at 37˚C for 20 min. After incubation, tissues were washed with neuronal medium [Minimum Essential Medium (Sigma) containing 10% horse serum (Sigma), N-2 supplement (1:100, Gibco, Grand Island, NY), 20 mM D-glucose, penicillin/streptomycin (1:500, Sigma), and 25 mM HEPES pH 7.5] and gently triturated 11 times by passing through a Pasteur pipette in 2 ml neuronal medium. The dissociated cells were passed through a 40-μm cell strainer (BD Falcon, San Diego, CA) and plated at $5x10^4$ and $4x10^6$ cells in poly-L-lysin (Sigma)-coated 48-well plates and 10-cm dishes, respectively. After plating, neurons were cultured for 7 days.

Plasmids. The coding regions of human RCAN1-1 (GenBank accession no. NM_004414) and FBW4 (GenBank accession no. AF281859) were amplified by PCR using human cDNA originating from the fetal brain and the liver (OriGene Technologies, Rockville, MD) as a template, respectively. That of human RCAN1-4 (GenBank accession no. NM_203418) was amplified by RT-PCR using total RNA from HEK293T cells as a template. Each PCR reaction used the following primer pairs: RCAN1-1, RCAN1-1f (5'-GGA TCCAAATGGAGGACGGCGTGGCCGG-3') and RCAN1r (5'-CCGCTCGAGTTCAGCTGAGGTGGATCGGCGTGT-3'); RCAN1-4, RCAN1-4f (5'-CGGGATCCAGATGCATT TTAGAAACTT-3') and RCAN1r, FBW4: FBW4f (5'-CGG AATTCTATGGCGGCGGCGGCCGGGGA-3') and FBW4r (5'-GCTCTAGATCATGGGTTTTGAAAATCCAGGACG TGG-3'). PCR products amplified using the primer pairs of RCAN1-1 and RCAN1-4 were inserted into *Bam*HI and *Xho*I of pcDNA3 tagged with the FLAG epitope (pcDNA3-FLAG), and those amplified using the primer pair of FBW4 were inserted into *Bam*HI and *Xba*I of pUHD-P2 tagged with the HA epitope (pUHD-P2-HA). The expression plasmids of HA-ß-TrCP1, HA-ß-TrCP2, myc-Rbx1 and FLAG-SKP1 were donated by Dr N. Watanabe (RIKEN) (40). pcDNA3-myc-Cul1 and pcDNA3.1-HA-ubiquitin were donated by Dr K.I. Nakayama (Kyushu University) and Dr T. Chiba (Tokyo Metropolitan Institute of Medical Science), respectively (41,42).

Transfection of expression plasmid. HEK293T cells were plated at $3x10^4$ cells and $1x10^5$ cells in 24-well plates and 10-cm dishes, respectively, and incubated for 10 h. Cells were transfected with DNA using GeneJuice Transfection Reagent

(Novagen). The total amount of DNA was kept at 250 ng and 5 μg by the addition of empty plasmid to 24-well plates and 10-cm dishes, respectively. After 10 h, the transfection mixture was replaced with fresh culture medium and incubated for an additional 2 h.

Small interference RNA. Small interference RNA (siRNA) for ß-TrCP1/2 was custom synthesized by Dharmacon (Lafayette, CO). The target sequence of siRNA for ß-TrCP1/2 was described previously (40). As a control, siCONTROL non-targeting siRNA #2 (Dharmacon) was used. Transfection of siRNA was performed by the reverse transfection method with Lipofectamine RNAiMax (Invitrogen, Carlsbad, CA), according to the manufacturer's instructions. Briefly, siRNA was added to 100 μl OPTI-MEM I (Gibco) in 24-well plates at a final concentration of 10 nM, and then incubated with 0.75 μl Lipofectamine RNAiMax for 20 min at room temperature. HEK293T cells were seeded at a density of $5x10^4$ cells into 24-well plates containing siRNA/transfection reagent complex. At 22 h after transfection, medium was replaced with fresh growth medium, and cells were incubated for another 2 h. In the case of the 6-cm dishes, it was performed with an 11-fold increase of all materials. We confirmed that ß-TrCP1/2 siRNA could inhibit >80% of the expression of ß-TrCP1 and ß-TrCP2 mRNAs in HEK293T cells under our experimental conditions.

Immunoprecipitation and re-immunoprecipitation. After stimulation with the indicated reagents, cells were washed with ice-cold PBS and lysed with lysis buffer [20 mM Tris-HCl pH 8.0, 150 mM NaCl, 10 mM ß-glycerophosphate, 5 mM NaF, 1 mM Na_3VO_4, 0.5% Nonidet P-40 and protease inhibitor cocktail (Complete, Roche)]. Cell lysates were rotated at 4˚C for 6 h and centrifuged at 20,630 x g for 15 min. The supernatant was used for immunoprecipitation with anti-FLAG M2 antibody-conjugated agarose (anti-FLAG M2 affinity gel, Eastman Kodak Co., Rochester, NY), or anti-HA (12CA5) or anti-RCAN1.2 antibody precoupled to protein G agarose (Santa Cruz Biotechnology, Santa Cruz, CA), and then immunoprecipitates were washed four times with M2 buffer (43). Re-immunoprecipitation (re-IP) was performed according to a previous method with minor modification (44). Briefly, immunoprecipitates with anti-FLAG M2 affinity gel were suspended in 100 μl SDS buffer and boiled at 95˚C for 10 min. Samples were stored at room temperature to cool and then centrifuged at 20,630 x g for 10 min at 20˚C. The supernatant was diluted in 1.1 ml TX-100 buffer and subjected to immunoprecipitation with anti-FLAG M2 affinity gel. After washing in M2 buffer, immunoprecipitates were dissolved in Laemmli buffer and 20 mM Tris-HCl buffer (pH 7.4) prior to immunoblotting and *in vitro* ubiquitination assay, respectively.

Immunoblotting. Samples were subjected to SDS-PAGE and transferred to polyvinylidene difluoride (PVDF) membranes (Millipore, Bedford, MA). Immunoblotting was performed with the indicated primary antibody and appropriate secondary antibody. Immunoreactive bands were visualized with ECL detection reagent (Amersham Life Science, Birmingham, UK) using a Lumivision Pro HSII image analyzer (Aisin Seiki, Aichi, Japan). Immunoblot images were saved as TIFF files, and pixel density was calculated for each band from TIFF files imported into YabGelImageX1.0.

In vitro ubiquitination assay and Western blotting with streptavidin-HRP. HEK293T cells were transfected with the expression plasmid of FLAG-RCAN1-1 or cotransfected with expression plasmids of SCF complex components (myc-Cul1, myc-Rbx, FLAG-Skp1 and either HA-ß-TrCP1 or HA-FBW4). Cells were stimulated with or without 5 mM H_2O_2 for 10 min, and cell lysates were prepared for immunoprecipitation with anti-FLAG M2 or anti-HA (12CA5) antibody. Immunoprecipitates were washed four times with M2 buffer and once with 20 mM Tris-HCl buffer (pH 7.4), and then subjected to *in vitro* ubiquitination assay (Ubiquitinylation Kit, Biomol Research Laboratories, Plymouth Meeting, PA), according to the manufacturer's instructions with minor modification. Briefly, E1, E2 and the immunoprecipitated SCF complex were added to the immunoprecipitated RCAN1-1 in ubiquitinylation reaction buffer including biotinylated ubiquitin and the ATP regeneration system. The reaction mixture was incubated at 30˚C for 1.5 h and then terminated by washing with M2 buffer four times. Immunoprecipitates were dissolved in Laemmli (IP samples) or SDS buffer. Samples dissolved in SDS buffer were further used for re-immunoprecipitation (re-IP samples). IP and re-IP samples were subjected to SDS-PAGE and transferred to a PVDF membrane. The membrane was blocked with 1% BSA/0.1% Tween-20/TBS (TBS-T) for 1 h and washed three times with TBS-T for 10 min. Streptavidin-HRP (Vectastatin ABC Elite Kit, Vector Laboratories, Burlingame, CA) was prepared according to the manufacturer's instructions and diluted 1:30 with 1% BSA/TBS-T. The membrane was incubated with diluted streptavidin-HRP for 2 h and then washed six times with TBS-T. Detection was carried out using ECL detection reagent.

Cellular fractionation. HEK293T cells were seeded on 6-cm dishes and transfected with siRNA. At 24 h after transfection, cells were stimulated with or without 5 mM H_2O_2 for 30 min and washed with ice-cold PBS followed by addition of 100 μl hypotonic buffer (20 mM Tris-HCl pH 8.0, 10 mM NaCl, 1 mM EDTA, 1 mM DTT, 0.2 mM sodium orthovanadate and 5 mM NaF). Cells were harvested and incubated on ice for 15 min with frequent vortexing. After incubation, cells were centrifuged at 1000 x g for 10 min. The pellet was resuspended in 100 μl extraction buffer I (ProteoExtract Subcellular Proteome Extraction Kit, Calbiochem) and rotated at 4˚C for 10 min followed by centrifugation at 1000 x g for 10 min. Each supernatant obtained by incubation with hypotonic buffer and extraction buffer I was collected together and centrifuged at 20,630 x g for 10 min. The resulting supernatant was used as the cytosolic fraction. The pellet obtained from extraction buffer I was resuspended in 100 μl extraction buffer II and rotated for 60 min followed by centrifugation at 6000 x g for 10 min. The pellet was resuspended in 50 μl extraction buffer III. Samples were rotated for 10 min and centrifuged at 6800 x g for 10 min. The supernatant was used as the nuclear fraction. Each protein fraction was added to four volumes of ice-cold

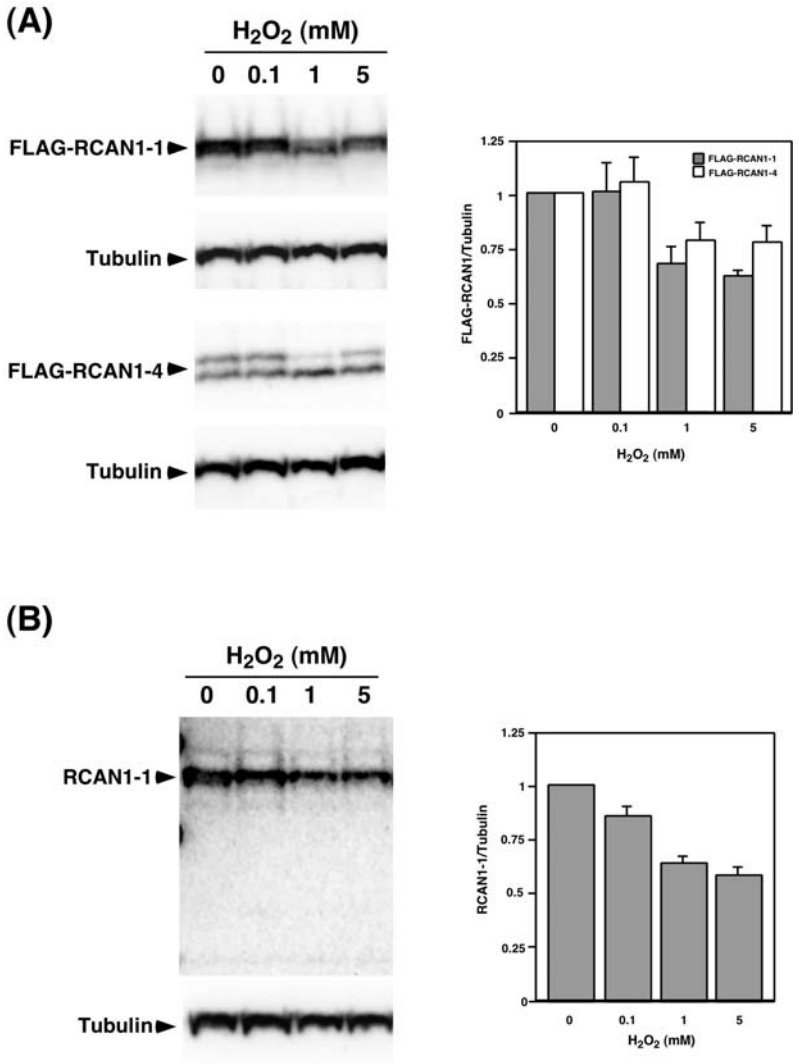

Figure 1. H_2O_2-induced decrease in RCAN1 in HEK293T cells. (A) HEK293T cells were transfected with the expression plasmid of FLAG-RCAN1-1 or FLAG-RCAN1-4. After transfection, cells were stimulated with the indicated concentration of H_2O_2 for 1 h. Samples were subjected to immunoblotting with anti-FLAG antibody followed by reprobing with anti-α-tubulin antibody. The band intensities of FLAG-RCAN1-1 and FLAG-RCAN1-4 were normalized against the corresponding tubulin band intensity. These values were presented on a bar graph as the relative amount to that of an unstimulated sample. Values are the mean ± SE. (B) At 24 h after seeding, cells were stimulated with the indicated concentration of H_2O_2 for 1 h. Samples were subjected to immunoblotting with anti-RCAN1.2 antibody followed by reprobing with anti-α-tubulin antibody. The band intensity of RCAN1-1 was normalized against the corresponding tubulin band intensity and presented on a bar graph, as described in A.

acetone and incubated on ice for 15 min followed by centrifugation at 12,000 x g for 10 min. The pellet was dissolved in Laemmli buffer and subjected to immunoblotting.

Results

H_2O_2-induced decrease in RCAN1-1 and RCAN1-4. We examined whether the protein level of RCAN1 is changed by H_2O_2 stimulation in HEK293T cells. As shown in Fig. 1A, H_2O_2 induced a decrease in FLAG-RCAN1-1 and FLAG-RCAN1-4 at higher concentrations of H_2O_2 (33±8 and 39±3% reduction of the FLAG-RCAN1-1 protein level at 1 and 5 mM H_2O_2, respectively; 22±6 and 23±6% reduction of FLAG-RCAN1-4 at 1 and 5 mM H_2O_2, respectively). As shown in Fig. 1B, endogenous RCAN1-1 was also decreased by H_2O_2 stimulation with the same dose dependency as that for the decrease in FLAG-RCAN1-1 (37±3 and 42±4% reduction of the endogenous RCAN1-1 protein level at 1 and 5 mM H_2O_2, respectively).

H_2O_2-induced ubiquitination of RCAN1. To assess whether or not the H_2O_2-induced decrease in RCAN1 is mediated by ubiquitination, we examined the occurrence of the covalent attachment of ubiquitin to RCAN1 in response to H_2O_2 stimulation, using the method of re-immunoprecipitation (re-IP). Non-covalently bound proteins can be removed from re-IP samples by secondary immunoprecipitation using boiled first immunoprecipitates. As shown in Fig. 2A, immunoblotting with anti-HA antibody showed that a high molecular weight smear band was detected in the immunoprecipitates of FLAG-RCAN1-1 from cells with stimulation by higher concentrations of H_2O_2 (1-5 mM). Immunoprecipitates of FLAG-RCAN1-4 with stimulation by higher concentrations

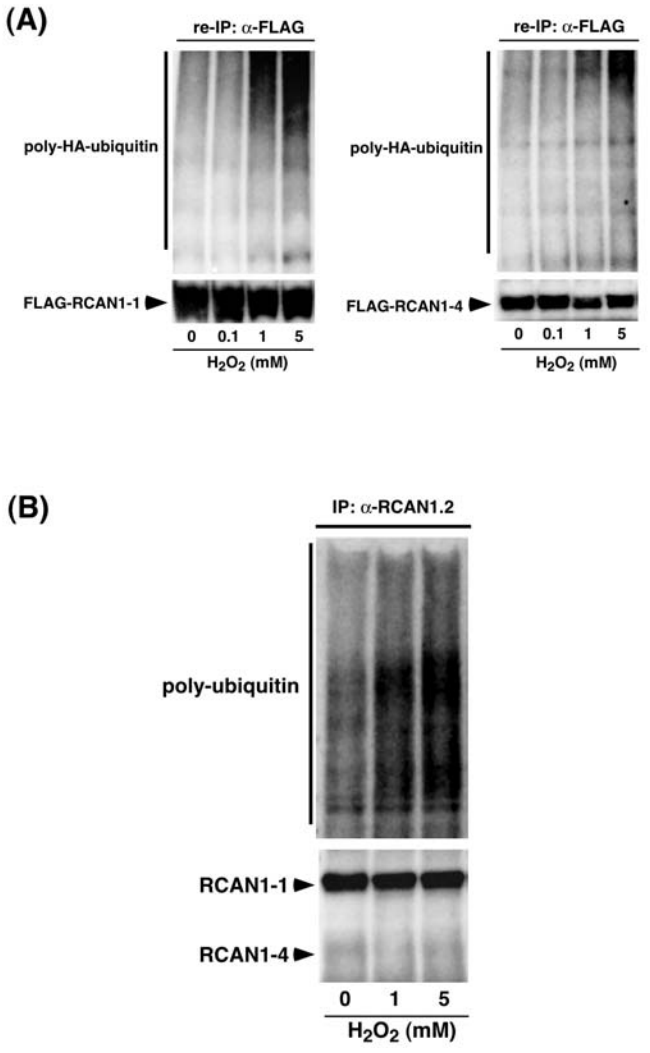

Figure 2. H_2O_2 induced ubiquitination of RCAN1 in a dose-dependent manner. (A) HEK293T cells were cotransfected with the expression plasmids of HA-ubiquitin and either FLAG-RCAN1-1 or FLAG-RCAN1-4. After transfection, cells were treated with 10 μM MG132 for 2 h and stimulated with the indicated concentration of H_2O_2 for 1 h. Cell lysates were used for immunoprecipitation with anti-FLAG M2 antibody. Immunoprecipitates were boiled for 10 min and then re-immunoprecipitated with anti-FLAG M2 antibody (re-IP). Re-IP samples were subjected to immunoblotting with anti-HA (3F10) antibody (upper panels). The accuracy of immunoprecipitation was assessed by reprobing with anti-FLAG M2 antibody (lower panels). (B) At 22 h after seeding, HEK293T cells were treated with 10 μM MG132 for 2 h and stimulated with the indicated concentration of H_2O_2 for 1 h. Then, cell lyates were used for immunoprecipitation with anti-RCAN1.2 antibody and immunoprecipitates were subjected to immunoblotting with anti-multi-ubiquitin antibody (upper panel) followed by reprobing with anti-RCAN1.2 antibody (lower panel).

of H_2O_2 (1-5 mM) were also detected in the smear band by immunoblotting. The appearance of the smear band was more typical with treatment with 5 mM H_2O_2 than that with 1 mM H_2O_2. As shown in Fig. 2B, the high molecular weight smear band was increased in endogenous RCAN1 immunoprecipitates with stimulation by higher concentrations of H_2O_2 (1-5 mM). These results suggest that H_2O_2 induces the ubiquitination of RCAN1 at higher concentrations of H_2O_2.

Identification of E3 ubiquitin ligase for RCAN1-1 dependent on H_2O_2 stimulation. To identify the E3 ubiquitin ligase specific for RCAN1 under H_2O_2 stimulation, we examined the interaction of RCAN1-1 with an F-box protein, a component of the SCF ubiquitin ligase. As shown in Fig. 3A, ß-TrCP1, a member of the F-box protein family, was clearly coimmunoprecipitated with RCAN1-1 in response to H_2O_2 stimulation. A small amount of ß-TrCP2 was also coimmunoprecipitated with FLAG-RCAN1-1 in response to H_2O_2. Although FBW4, another member of the F-box protein family, was coimmunoprecipitated with RCAN1-1, the interaction of FBW4 with RCAN1-1 was independent of H_2O_2 stimulation. Then, to assess whether $SCF^{ß\text{-}TrCP}$ mediates ubiquitination of RCAN1-1 dependent on H_2O_2 stimulation, we performed an *in vitro* ubiquitination assay. As shown in Fig. 3B (left panel), $SCF^{ß\text{-}TrCP1}$ significantly increased the accumulation of a high molecular weight smear band characteristic of poly-ubiquitin in immunoprecipitates of FLAG-RCAN1-1 from H_2O_2-stimulated cells compared to the control. On the other hand, SCF^{FBW4} induced accumulation of the smear band in immunoprecipitates of FLAG-RCAN1-1, but its accumulation was independent of H_2O_2 stimulation (Fig. 3B, right panel). To further assess whether the $SCF^{ß\text{-}TrCP1}$-mediated high molecular weight smear specifically resulted from poly-ubiquitinated FLAG-RCAN1-1, immunoprecipitates of FLAG-RCAN1-1 were subjected to re-IP after the ubiquitination reaction with $SCF^{ß\text{-}TrCP1}$ to exclude other interacting molecules. As shown in Fig. 3C, $SCF^{ß\text{-}TrCP1}$ induced accumulation of the smear band of FLAG-RCAN1-1 in H_2O_2-stimulated cells compared to the control in re-IP samples. These results indicate that RCAN1-1 is ubiquitinated by $SCF^{ß\text{-}TrCP1}$ in response to H_2O_2 stimulation *in vitro*.

Effect of ß-TrCP1/2 siRNA on the H_2O_2-induced decrease in RCAN1. To investigate whether $SCF^{ß\text{-}TrCP}$ functions as an E3 ubiquitin ligase for RCAN1 under H_2O_2 stimulation in HEK293T cells, we examined the effect of ß-TrCP1/2 knockdown on the H_2O_2-induced decrease in RCAN1. As shown in Fig. 4A, ß-TrCP1/2 siRNA but not control siRNA abolished the H_2O_2-induced decrease in RCAN1-1. To further evaluate the cellular compartment in which RCAN1 is ubiquitinated by $SCF^{ß\text{-}TrCP}$, we examined the effect of ß-TrCP1/2 siRNA on the protein level of RCAN1 in the subcellular fractions. As shown in Fig. 4B, ß-TrCP1/2 siRNA abolished the H_2O_2-induced decrease in RCAN1-1 in the cytosolic and nuclear fractions. In addition, immunoblotting using the nuclear fraction showed that endogenous RCAN1-4 was decreased by H_2O_2 stimulation, which was abolished by ß-TrCP1/2 siRNA. These results suggest that $SCF^{ß\text{-}TrCP}$ mediated the H_2O_2-induced decrease in RCAN1-1 in the cytosol and nucleus and that of RCAN1-4 in the nucleus of HEK293T cells.

H_2O_2-induced ubiquitination of RCAN1-1 in primary neurons. RCAN1 is expressed in the hippocampus and cerebral cortex of the human brain (4). Neurons are sensitive to oxidative stress. Therefore, we investigated whether H_2O_2 induces ubiquitination of RCAN1 in primary neurons, similarly to

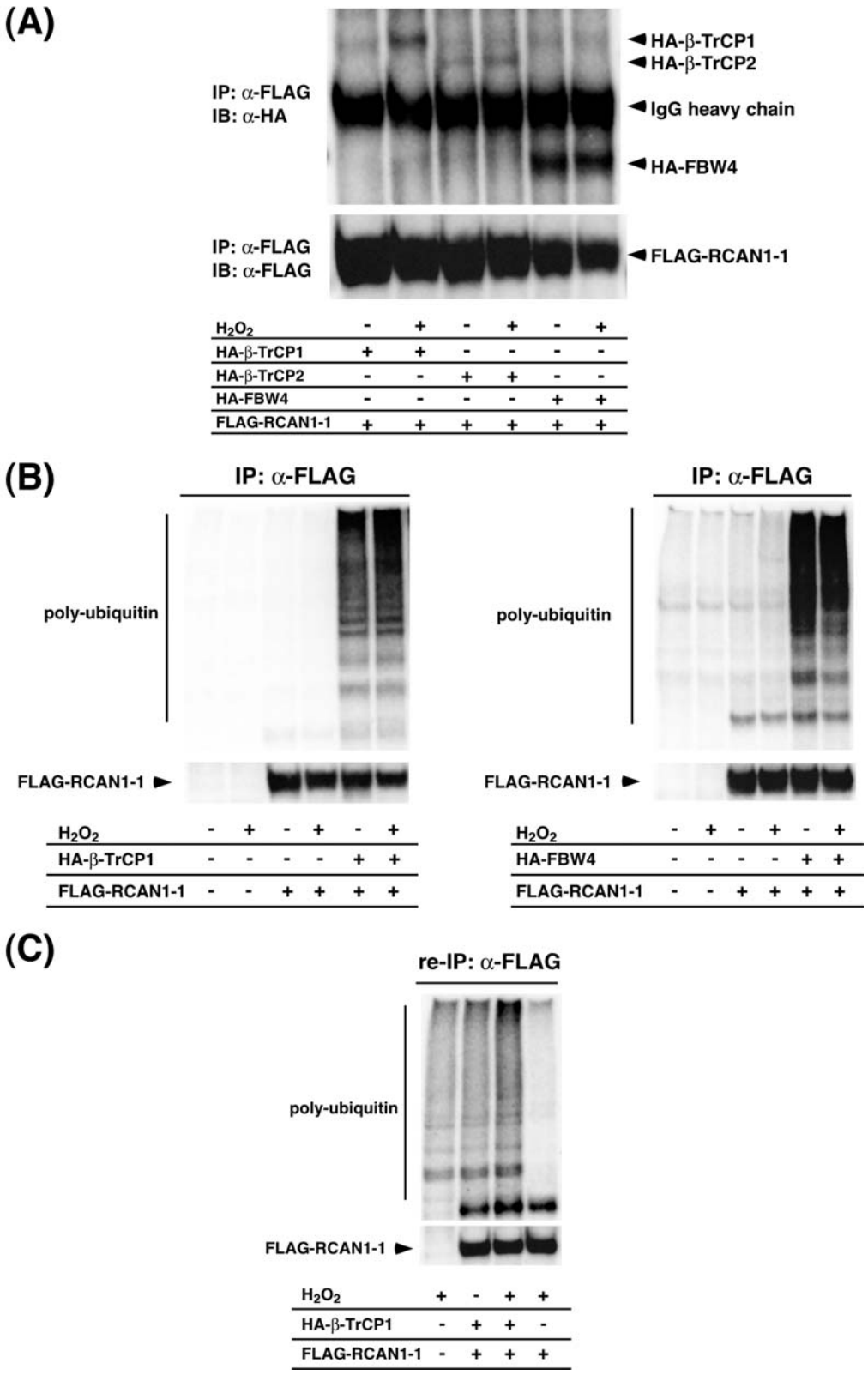

Figure 3. Identification of E3 ubiquitin ligase for RCAN1-1 dependent on H_2O_2 stimulation. (A) HEK293T cells were cotransfected with the expression plasmids of FLAG-RCAN1-1 and either HA-ß-TrCP1, HA-ß-TrCP2 or HA-FBW4. After transfection, cells were stimulated with or without 5 mM H_2O_2 for 15 min and then the reaction was terminated. Cell lysates were used for immunoprecipitation (IP) with anti-FLAG M2 antibody, and immunoprecipitates were subjected to immunoblotting (IB) with anti-HA (12CA5) antibody (upper panel) followed by reprobing with anti-FLAG M2 antibody (lower panel). (B) HEK293T cells expressing FLAG-RCAN1-1 or SCF complex components including HA-ß-TrCP1 or HA-FBW4 were stimulated with or without 5 mM H_2O_2 for 10 min. Cell lysates were used for immunoprecipitation with anti-FLAG M2 or anti-HA (12CA5) antibody, and each immunoprecipitate was subjected to *in vitro* ubiquitination assay with biotinylated ubiquitin. After ubiquitination reaction, immunoprecipitates (IP) were terminated by adding Laemmli buffer. IP samples were subjected to Western blotting with streptavidin-HRP followed by reprobing with anti-FLAG M2 antibody. (C) HEK293T cells expressing FLAG-RCAN1-1 or SCF complex components including HA-ß-TrCP1 were stimulated with or without 5 mM H_2O_2 for 10 min. Immunoprecipitates were prepared and used for *in vitro* ubiquitination assay. After the ubiquitination reaction, samples were boiled for 10 min at 95˚C and then used for re-immunoprecipitation with anti-FLAG M2 antibody (re-IP). The re-IP samples were subjected to Western blotting, as described in B.

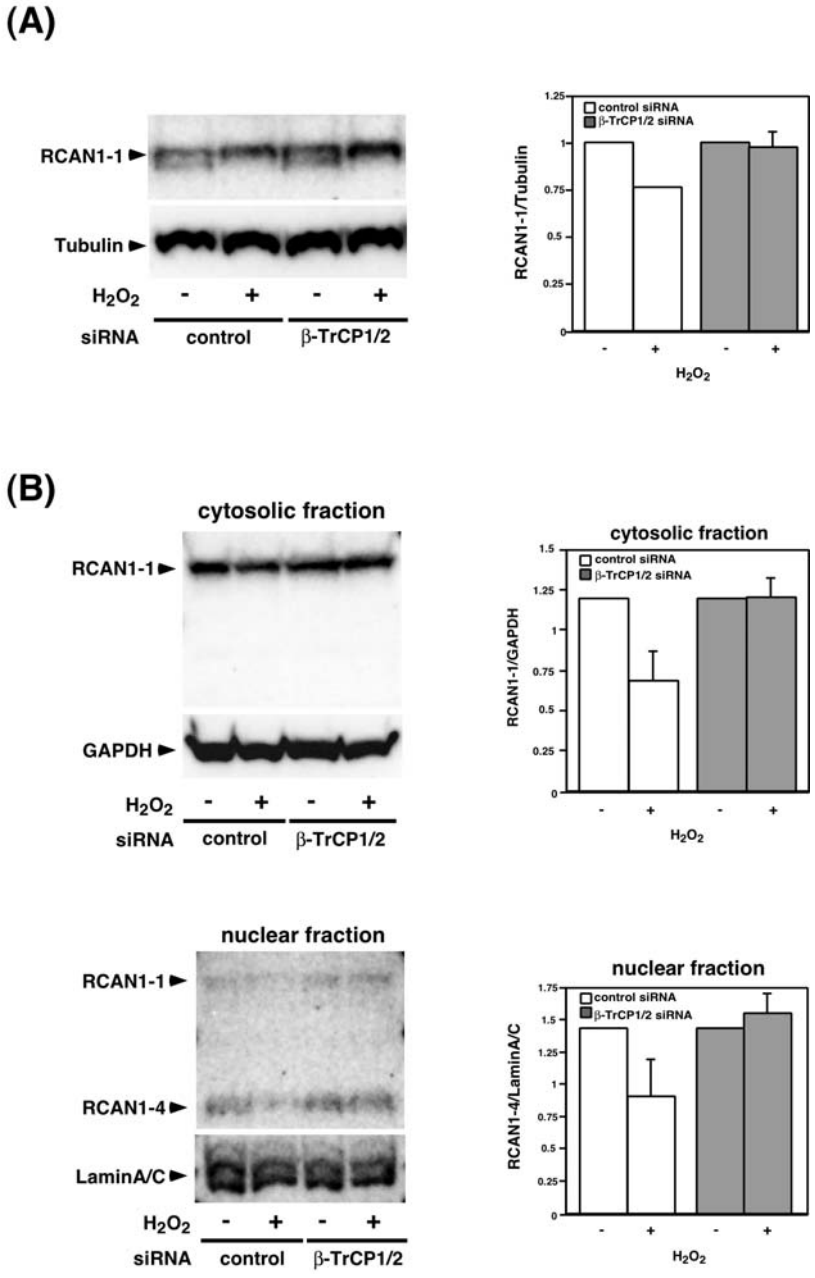

Figure 4. Effect of ß-TrCP1/2 siRNA on H_2O_2-induced decrease in RCAN1. (A) The indicated siRNAs were introduced into HEK293T cells on 24-well plates by reverse transfection method. After transfection, cells were stimulated with or without 5 mM H_2O_2 for 1 h and lysed with Laemmli buffer. Samples were subjected to immunoblotting with anti-RCAN1.2 antibody (upper panel) followed by reprobing with anti-α-tubulin antibody (lower panel). The band intensity of RCAN1-1 was normalized against the corresponding tubulin band intensity and presented on a bar graph as the relative amount to that of an unstimulated sample. Values are the mean ± SE. (B) The indicated siRNA was introduced into HEK293T cells on 6-cm dishes by reverse transfection method. After transfection, cells were stimulated with or without 5 mM H_2O_2 for 30 min and then hypotonic buffer was added. Cells were harvested and divided into cytosolic and nuclear fractions. Each protein fraction was subjected to immunoblotting with anti-RCAN1.2 antibody, followed by reprobing with anti-GAPDH or anti-laminA/C antibody as an internal control for each fraction. The band intensities of RCAN1-1 in the cytosolic fraction and RCAN1-4 in the nuclear fraction were normalized against the corresponding internal control band intensity and presented on a bar graph, as described in A.

that in HEK293T cells. As shown in Fig. 5A, H_2O_2 induced a decrease in RCAN1 at higher concentrations for up to 2 h in hippocampal and cortical neurons (50-500 μM and 100-500 μM in hippocampal and cortical neurons, respectively). A previous study demonstrated that RCAN1 is cleaved through calpain, the Ca^{2+}-activated protease, by exposure to 50 μM H_2O_2 in cerebellar cortex neurons (19). Then, we assessed whether or not the H_2O_2-induced decrease in RCAN1-1 was mediated by calpain in these neurons. As shown in Fig. 5B, 100 μM PD150606, an inhibitor of calpain I and II, prevented the decrease in RCAN1-1 by stimulation with 100 μM H_2O_2 in hippocampal and cortical neurons. However, PD150606 failed to inhibit the decrease in RCAN1-1 at higher concentrations of H_2O_2 (>200 and 500 μM in hippocampal and cortical neurons, respectively). Therefore, we investigated whether RCAN1 is ubiquitinated by stimulation with 100 and 500 μM H_2O_2, concentrations at which PD150606 has a different inhibitory effect on the H_2O_2-induced decrease in RCAN1-1

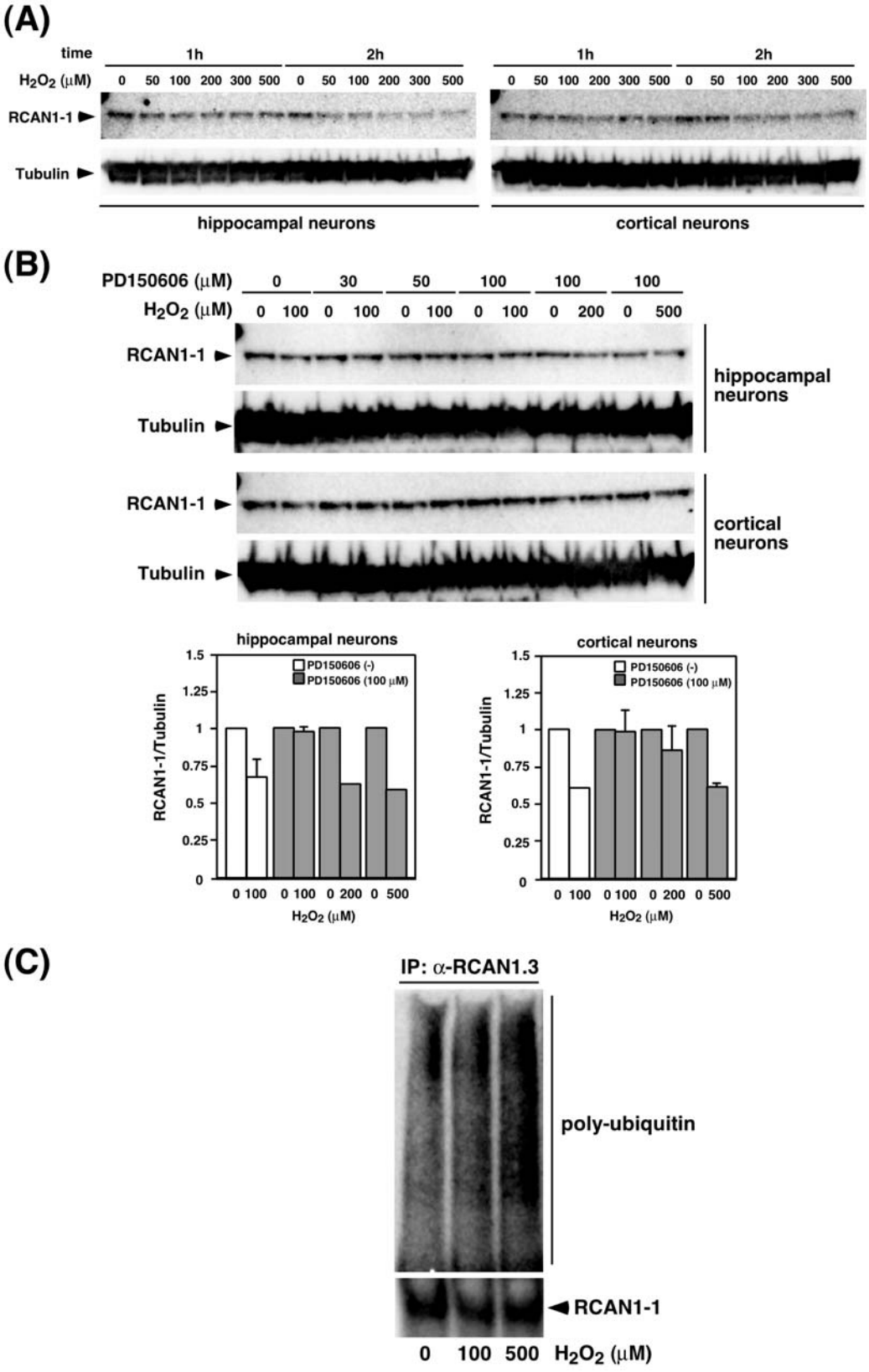

Figure 5. H_2O_2-induced ubiquitination of RCAN1 in primary neurons. (A) Primary hippocampal and cortical neurons were stimulated with the indicated concentration of H_2O_2 for 1 or 2 h, and lysed with Laemmli buffer. Samples were subjected to immunoblotting with anti-RCAN1.3 antibody (upper panels), followed by reprobing with anti-neuronal class III ß-tubulin antibody (lower panels). (B) Primary hippocampal and cortical neurons were treated with or without PD150606, a calpain inhibitor, for 1 h followed by stimulation with H_2O_2 for 1 h and lysed with Laemmli buffer. Samples were subjected to immunoblotting with anti-RCAN1.3 antibody (upper panels), followed by reprobing with anti-neuronal class III ß-tubulin antibody (lower panels). RCAN1-1 band intensities of 0 and 100 μM PD150606-treated samples were normalized against the corresponding tubulin band intensity and presented on a bar graph as the relative amount to that of each unstimulated sample. Values are the mean ± SE. (C) Cortical neurons were treated with 10 μM MG132 for 2 h and then stimulated with the indicated concentration of H_2O_2 for 1 h. The reaction was terminated by adding lysis buffer, and cell lysates were immunoprecipitated with anti-RCAN1.3 antibody. Immunoprecipitates were subjected to immunoblotting with anti-multi-ubiquitin antibody (upper panel), followed by reprobing with anti-RCANA1.3 antibody (lower panel).

in cortical neurons. As shown in Fig. 5C, the high molecular weight smear band was increased in RCAN1 immunoprecipitates from cortical neurons with stimulation by 500 μM H_2O_2 compared to those of the control and stimulation by 100 μM H_2O_2. These results suggest that H_2O_2 induced a decrease in RCAN1-1 via the ubiquitin pathway at the higher concentrations.

Discussion

RCAN1 was ubiquitinated by the same concentrations of H_2O_2 as those for the H_2O_2-induced decrease in RCAN1, suggesting that the decrease in RCAN1 was caused by ubiquitination of RCAN1 (Figs. 1 and 2). Then, to explore the mechanism of the H_2O_2-induced decrease in RCAN1 through the UPS, we investigated the E3 ubiquitin ligase for RCAN1 under H_2O_2 stimulation. As shown in Fig. 3A, ß-TrCP1 and ß-TrCP2 interacted with RCAN1-1 in response to stimulation with H_2O_2. On the other hand, the interaction of FBW4 with RCAN1-1 was independent of H_2O_2 stimulation. The results of the interaction between RCAN1-1 and F-box protein correlated with those of the *in vitro* ubiquitination assay. $SCF^{ß\text{-}TrCP}$ increased poly-ubiquitination of RCAN1-1 dependent on H_2O_2 stimulation in both IP and re-IP samples (Fig. 3B, left panel and C). However, SCF^{FBW4}-induced poly-ubiquitination of RCAN1-1 was independent of H_2O_2 stimulation (Fig. 3B, right panel). These results suggest that H_2O_2-induced ubiquitination of RCAN1-1 is mediated by $SCF^{ß\text{-}TrCP}$. The experiments using ß-TrCP1/2 siRNA supported this suggestion. As shown in Fig. 4B, ß-TrCP1/2 siRNA abolished the H_2O_2-induced decrease in RCAN1-1 in the cytosol and nucleus and that of RCAN1-4 in the nucleus. Taken together, these results indicate that H_2O_2 induced ubiquitination of RCAN1 via $SCF^{ß\text{-}TrCP}$, resulting in a decrease in the protein level of RCAN1 in HEK293T cells.

It was reported that RCAN1-1 and RCAN1-4 have increased stability in the presence of MG132 and that overexpressed exogenous RCAN1-4 is ubiquitinated under normal culture conditions (35,36,45). Our previous study demonstrated that the *Saccharomyces cerevisiae* ortholog of RCAN1 is ubiquitinated by SCF^{Cdc4} in response to a rise in intracellular Ca^{2+} (34). It may be possible that RCAN1-1 and RCAN1-4 are ubiquitinated by another E3 ubiquitin ligase, such as SCF^{FBW7}, human ortholog of SCF^{Cdc4}, and SCF^{FBW4}, under different conditions than oxidative stress. FBW4 is known as dactylin, and its gene is localized within the Split Hand-Split Foot malformation (SHFM) 3 critical region (46,47). Dactylin-disrupted mice present malformed single digits and a lack of fore and hind paws in homozygotes. It is likely that RCAN1 could be involved in the developmental patterning of the limbs.

RCAN1-1 and RCAN1-4 exhibited different subcellular distributions. RCAN1-1 was largely distributed in the cytosol with little in the nucleus, and RCAN1-4 was distributed in the nucleus in HEK293T cells. A 24-kDa band corresponding to RCAN1-4 in whole cell lysates could not be detected with anti-RCAN1.2 antibody, but it was detected in nuclear protein extracts (Figs. 1B and 5B). It may be difficult to detect RCAN1-4 in immunoblotting using whole cell lysates because of the low expression level of RCAN1-4 localized in the nucleus.

RCAN1 has been implicated in physiological and pathological responses in neurons. Thus, we investigated whether H_2O_2 induces ubiquitination of RCAN1 in primary neurons. As shown in Fig. 5B, 500 μM H_2O_2 induced a calpain-independent decrease in RCAN1-1 in neurons. In addition, the same concentration of H_2O_2 also induced ubiquitination of RCAN1 (Fig. 5C). These results suggest that a higher concentration of H_2O_2 induces a decrease in RCAN1-1 through the ubiquitin pathway. Neurons in RCAN1 knockout mice exhibit more resistance to H_2O_2-induced cell death than wild-type neurons (19). In this study, more than 1 mM and 500 μM H_2O_2 finally led to cell death after 2 and 6 h of stimulation in HEK293T cells and primary neurons, respectively (data not shown). Ubiquitin-mediated degradation of RCAN1 may be required for the survival response to oxidative stress.

Based on our findings, oxidative stress induces a ubiquitin-mediated decrease in RCAN1. However, RCAN1 is increased in the brains of Alzheimer's disease patients (AD), where oxidative stress is involved in the pathogenic process (4,31,32). Previous findings have shown the deposition of ubiquitinated proteins by impairment of the UPS in neurodegenerative diseases including AD (29,30). We hypothesized that impairment of the UPS in AD might lead to the accumulation of ubiquitinated RCAN1 by oxidative stress, resulting in a change in Cn activity and resistance to damage by oxidative stress. To verify the hypothesis, further studies are needed.

In this study, we demonstrated that RCAN1 is a target of $SCF^{ß\text{-}TrCP}$ and that H_2O_2 induces $SCF^{ß\text{-}TrCP}$-mediated ubiquitination of RCAN1, leading to its decrease. These results suggest that degradation of RCAN1 by the ubiquitin pathway may be an important event in oxidative stress-induced cellular responses, including cell death.

Acknowledgements

We thank Dr Wendy Gray for the editorial assistance. We thank the following individuals for the expression plasmids: Dr Nobumoto Watanabe for HA-ß-TrCP1, HA-ß-TrCP2, myc-Rbx1 and FLAG-SKP1; Dr Keiichi Nakayama for myc-Cul1; Dr Tomoki Chiba for HA-ubiquitin. We also thank Drs Masashi Ueki, Noriko Koyama, Junji Fukada and Yusuke Yoshida for the helpful discussion and Ms Satomi Yamamoto and Ms. Noriko Watanabe for the technical support. This work was supported by a Grant-in-Aid for Young Scientists (B) (19790221 to S.A.) from the Ministry of Education, Culture, Sports, Science and Technology of Japan and a grant from RIKEN (to T.K.).

References

1. Fuentes JJ, Pritchard MA, Planas AM, Bosch A, Ferrer I and Estivill X: A new human gene from the Down syndrome critical region encodes a proline-rich protein highly expressed in fetal brain and heart. Hum Mol Genet 4: 1935-1944, 1995.
2. Fuentes JJ, Pritchard MA and Estivill X: Genomic organization, alternative splicing, and expression patterns of the DSCR1 (Down syndrome candidate region 1) gene. Genomics 44: 358-361, 1997.
3. Ermak G, Harris CD, Battocchio D and Davies KJ: RCAN1 (DSCR1 or Adapt78) stimulates expression of GSK-3beta. FEBS J 273: 2100-2109, 2006.

4. Ermak G, Morgan TE and Davies KJ: Chronic overexpression of the calcineurin inhibitory gene DSCR1 (Adapt78) is associated with Alzheimer's disease. J Biol Chem 276: 38787-38794, 2001.
5. Kingsbury TJ and Cunningham KW: A conserved family of calcineurin regulators. Genes Dev 14: 1595-1604, 2000.
6. Gorlach J, Fox DS, Cutler NS, Cox GM, Perfect JR and Heitman J: Identification and characterization of a highly conserved calcineurin binding protein, CBP1/calcipressin, in Cryptococcus neoformans. EMBO J 19: 3618-3629, 2000.
7. Vega RB, Yang J, Rothermel BA, Bassel-Duby R and Williams RS: Multiple domains of MCIP1 contribute to inhibition of calcineurin activity. J Biol Chem 277: 30401-30407, 2002.
8. Iizuka M, Abe M, Shiiba K, Sasaki I and Sato Y: Down syndrome candidate region 1, a downstream target of VEGF, participates in endothelial cell migration and angiogenesis. J Vasc Res 41: 334-344, 2004.
9. Cho YJ, Abe M, Kim SY and Sato Y: Raf-1 is a binding partner of DSCR1. Arch Biochem Biophys 439: 121-128, 2005.
10. Stewart AA, Ingebritsen TS, Manalan A, Klee CB and Cohen P: Discovery of a Ca^{2+}- and calmodulin-dependent protein phosphatase: probable identity with calcineurin (CaM-BP80). FEBS Lett 137: 80-84, 1982.
11. Klee CB and Krinks MH: Purification of cyclic 3',5'-nucleotide phosphodiesterase inhibitory protein by affinity chromatography on activator protein coupled to Sepharose. Biochemistry 17: 120-126, 1978.
12. Klee CB, Krinks MH, Manalan AS, Cohen P and Stewart AA: Isolation and characterization of bovine brain calcineurin: a calmodulin-stimulated protein phosphatase. Methods Enzymol 102: 227-244, 1983.
13. Klee CB, Ren H and Wang X: Regulation of the calmodulin-stimulated protein phosphatase, calcineurin. J Biol Chem 273: 13367-13370, 1998.
14. Fuentes JJ, Genesca L, Kingsbury TJ, Cunningham KW, Perez-Riba M, Estivill X and de la Luna S: DSCR1, overexpressed in Down syndrome, is an inhibitor of calcineurin-mediated signaling pathways. Hum Mol Genet 9: 1681-1690, 2000.
15. Rothermel BA, McKinsey TA, Vega RB, Nicol RL, Mammen P, Yang J, Antos CL, Shelton JM, Bassel-Duby R, Olson EN and Williams RS: Myocyte-enriched calcineurin-interacting protein, MCIP1, inhibits cardiac hypertrophy in vivo. Proc Natl Acad Sci USA 98: 3328-3333, 2001.
16. van Rooij E, Doevendans PA, Crijns HJ, Heeneman S, Lips DJ, van Bilsen M, Williams RS, Olson EN, Bassel-Duby R, Rothermel BA and De Windt LJ: MCIP1 overexpression suppresses left ventricular remodeling and sustains cardiac function after myocardial infarction. Circ Res 94: e18-e26, 2004.
17. Sanna B, Brandt EB, Kaiser RA, Pfluger P, Witt SA, Kimball TR, van Rooij E, De Windt LJ, Rothenberg ME, Tschop MH, Benoit SC and Molkentin JD: Modulatory calcineurin-interacting proteins 1 and 2 function as calcineurin facilitators in vivo. Proc Natl Acad Sci USA 103: 7327-7332, 2006.
18. Ryeom S, Greenwald RJ, Sharpe AH and McKeon F: The threshold pattern of calcineurin-dependent gene expression is altered by loss of the endogenous inhibitor calcipressin. Nat Immunol 4: 874-881, 2003.
19. Porta S, Serra SA, Huch M, Valverde MA, Llorens F, Estivill X, Arbones ML and Marti E: RCAN1 (DSCR1) increases neuronal susceptibility to oxidative stress: a potential pathogenic process in neurodegeneration. Hum Mol Genet 16: 1039-1050, 2007.
20. Vega RB, Rothermel BA, Weinheimer CJ, Kovacs A, Naseem RH, Bassel-Duby R, Williams RS and Olson EN: Dual roles of modulatory calcineurin-interacting protein 1 in cardiac hypertrophy. Proc Natl Acad Sci USA 100: 669-674, 2003.
21. Ciechanover A, Heller H, Elias S, Haas AL and Hershko A: ATP-dependent conjugation of reticulocyte proteins with the polypeptide required for protein degradation. Proc Natl Acad Sci USA 77: 1365-1368, 1980.
22. Hershko A, Ciechanover A, Heller H, Haas AL and Rose IA: Proposed role of ATP in protein breakdown: conjugation of protein with multiple chains of the polypeptide of ATP-dependent proteolysis. Proc Natl Acad Sci USA 77: 1783-1786, 1980.
23. Hershko A, Heller H, Elias S and Ciechanover A: Components of ubiquitin-protein ligase system. Resolution, affinity purification, and role in protein breakdown. J Biol Chem 258: 8206-8214, 1983.
24. Kornitzer D and Ciechanover A: Modes of regulation of ubiquitin-mediated protein degradation. J Cell Physiol 182: 1-11, 2000.
25. Baumeister W, Walz J, Zuhl F and Seemuller E: The proteasome: paradigm of a self-compartmentalizing protease. Cell 92: 367-380, 1998.
26. Winston JT, Koepp DM, Zhu C, Elledge SJ and Harper JW: A family of mammalian F-box proteins. Curr Biol 9: 1180-1182, 1999.
27. Cenciarelli C, Chiaur DS, Guardavaccaro D, Parks W, Vidal M and Pagano M: Identification of a family of human F-box proteins. Curr Biol 9: 1177-1179, 1999.
28. Cardozo T and Pagano M: The SCF ubiquitin ligase: insights into a molecular machine. Nat Rev Mol Cell Biol 5: 739-751, 2004.
29. Taylor JP, Hardy J and Fischbeck KH: Toxic proteins in neurodegenerative disease. Science 296: 1991-1995, 2002.
30. de Vrij FM, Fischer DF, van Leeuwen FW and Hol EM: Protein quality control in Alzheimer's disease by the ubiquitin proteasome system. Prog Neurobiol 74: 249-270, 2004.
31. Barnham KJ, Masters CL and Bush AI: Neurodegenerative diseases and oxidative stress. Nat Rev Drug Discov 3: 205-214, 2004.
32. Behl C: Amyloid beta-protein toxicity and oxidative stress in Alzheimer's disease. Cell Tissue Res 290: 471-480, 1997.
33. Cook CN, Hejna MJ, Magnuson DJ and Lee JM: Expression of calcipressin1, an inhibitor of the phosphatase calcineurin, is altered with aging and Alzheimer's disease. J Alzheimers Dis 8: 63-73, 2005.
34. Kishi T, Ikeda A, Nagao R and Koyama N: The SCFCdc4 ubiquitin ligase regulates calcineurin signaling through degradation of phosphorylated Rcn1, an inhibitor of calcineurin. Proc Natl Acad Sci USA 104: 17418-17423, 2007.
35. Lee EJ, Lee JY, Seo SR and Chung KC: Overexpression of DSCR1 blocks zinc-induced neuronal cell death through the formation of nuclear aggregates. Mol Cell Neurosci 35: 585-595, 2007.
36. Ma H, Xiong H, Liu T, Zhang L, Godzik A and Zhang Z: Aggregate formation and synaptic abnormality induced by DSCR1. J Neurochem 88: 1485-1496, 2004.
37. Narayan AV, Stadel R, Hahn AB, Bhoiwala DL, Cornielle G, Sarazin E, Koleilat I and Crawford DR: Redox response of the endogenous calcineurin inhibitor Adapt 78. Free Radic Biol Med 39: 719-727, 2005.
38. McAllister AK: Biolistic transfection of neurons. Sci STKE 2000: pl1, 2000.
39. Hama H, Hara C, Yamaguchi K and Miyawaki A: PKC signaling mediates global enhancement of excitatory synaptogenesis in neurons triggered by local contact with astrocytes. Neuron 41: 405-415, 2004.
40. Watanabe N, Arai H, Nishihara Y, Taniguchi M, Watanabe N, Hunter T and Osada H: M-phase kinases induce phospho-dependent ubiquitination of somatic Wee1 by $SCF^{\beta\text{-}TrCP}$. Proc Natl Acad Sci USA 101: 4419-4424, 2004.
41. Yada M, Hatakeyama S, Kamura T, Nishiyama M, Tsunematsu R, Imaki H, Ishida N, Okumura F, Nakayama K and Nakayama KI: Phosphorylation-dependent degradation of c-Myc is mediated by the F-box protein Fbw7. EMBO J 23: 2116-2125, 2004.
42. Ebisawa T, Fukuchi M, Murakami G, Chiba T, Tanaka K, Imamura T and Miyazono K: Smurf1 interacts with transforming growth factor-beta type I receptor through Smad7 and induces receptor degradation. J Biol Chem 276: 12477-12480, 2001.
43. Asada S, Kasuya Y, Hama H, Masaki T and Goto K: Cyto-differentiation potentiates aFGF-induced $p21^{ras}$/Erk signaling pathway in rat cultured astrocytes. Biochem Biophys Res Commun 260: 441-445, 1999.
44. De Hoog CL, Koehler JA, Goldstein MD, Taylor P, Figeys D and Moran MF: Ras binding triggers ubiquitination of the Ras exchange factor Ras-GRF2. Mol Cell Biol 21: 2107-2117, 2001.
45. Genesca L, Aubareda A, Fuentes JJ, Estivill X, De La Luna S and Perez-Riba M: Phosphorylation of calcipressin 1 increases its ability to inhibit calcineurin and decreases calcipressin half-life. Biochem J 374: 567-575, 2003.
46. Ianakiev P, Kilpatrick MW, Dealy C, Kosher R, Korenberg JR, Chen XN and Tsipouras P: A novel human gene encoding an F-box/WD40 containing protein maps in the SHFM3 critical region on 10q24. Biochem Biophys Res Commun 261: 64-70, 1999.
47. Sidow A, Bulotsky MS, Kerrebrock AW, Birren BW, Altshuler D, Jaenisch R, Johnson KR and Lander ES: A novel member of the F-box/WD40 gene family, encoding dactylin, is disrupted in the mouse dactylaplasia mutant. Nat Genet 23: 104-107, 1999.